Optoelectronic Packaging for 16-Channel Optical Backplane Bus using Volume Hologram Optical Elements for High Performance Computing

Hai Bi, Jinho Choi, J. Ellis and R. T. Chen*
University of Texas at Austin
Microelectronic Research Center
10100 Burnet Road, Austin, Texas 78758
Email: chen@ece.utexas.edu

Abstract

Optical backplane bus not only can fulfill the ever increasing bandwidth demands in high performance computing but also allows the sharing of transmission medium to reduce wiring congestions. A 3-slot optical backplane bus demonstrator using photopolymer volume gratings array (PVGA) on top surface of glass substrate to fan-out light beam is designed to allow 16 channels of data to be exchanged between daughter slots and central slot. Alignment tolerance of the optical interconnect system is investigated theoretically and experimentally. By analyzing the diffractive characteristics, the 3dB bandwidth limit of the optical layer is determined to be more than 36nm. By carefully aligning the fabrication system, the incident angle deviation from Bragg condition is reduced to below 0.1°, much less than the 0.7° angular tolerance. The variation of the hologram efficiency is below 3dB by optimizing the recording beams.

In the optical sub-system, VCSELs and photodetectors packaged in the form of TO-46 can are assembled on top of each PVG and interleaved to reduce the crosstalk to below noise level. Three computer mother boards using FPGA are made to verify the data transmission among the slots. Interface boards between the FPGA boards and optical transceivers are designed and fabricated to separate the implementation of digital layer and optical layer. Above 4.8Gbps aggregated data transmission is successfully demonstrated using the multi-channel system. Single channel transmissions at 10Gbps data rate is also tested with above 100uW input power, showing the potential to improve the total two-way bandwidth to above 102.4Gbps

Keywords: optical bus, optical interconnect, alignment tolerance, multi-channel, volume grating array

I. INTRODUCTION

With the advent and popularity of multi-core and 64bit processors in High Performance Computing (HPC) systems, the demand on transferring data among multiple processing units inside a box is increasing rapidly [1]. The electrical backplane interconnects in the HPCs have abandoned bus architecture to overcome bandwidth limit of electrical bus and adopted point-to-point architecture which in turn causes wiring congestion crises and the difficulties to seat daughter boards onto backplane [2]. It was pointed out that optical interconnects possess potential advantage to avoid wiring congestion by using high speed bus to allow multiple boards to share transmission channels [3].

Based on the centralized architecture using volume polymer gratings with equalized fan-out power among boards, single channel memory to CPU interconnect [4] and interleaved optical interconnect with 15Gbps data rate [3] were demonstrated. Because of the 2D nature of the hologram film, the optical interconnect is anticipated to achieve Terahertz bandwidth inside an enclosure if multi-channel system can be built. Analysis of alignment tolerance is critical for optical system packaging and needs investigation.

In our work, the fully packaged optical sub-system was equipped with 4×8 Photopolymer Volume Gratings Array (PVGA) for each board, allowing us to investigate critical packaging issues such as angular misalignment tolerance and uniformity of gratings diffraction among channels. In the system diagram shown in Figure 1, the optical domain includes a glass substrate with volume hologram grating arrays on the surface and optoelectronics components. In the centralized architecture, the receivers on the central distributor board collect the signal from any daughter slot, and then deliver the information to the upper layer FPGA board for rebroadcast to daughter boards [4].

Layered design technology was used to separate the electronic domain with optical domain to reduce design difficulty. However, in the future, it will be preferred that lasers or modulators and drivers can be integrated into CMOS circuit or CMOS/BiCMOS circuits to improve the packing density. At current stage, individual O/E components are used to demonstrate the feasibility of the optical bus interconnect.

The demonstrated computer server system has three optoelectronically interconnected boards, each incorporated a FPGA with PowerPC core for supporting 32 channels of bit oriented data streams, 16 inbound and 16 outbound.

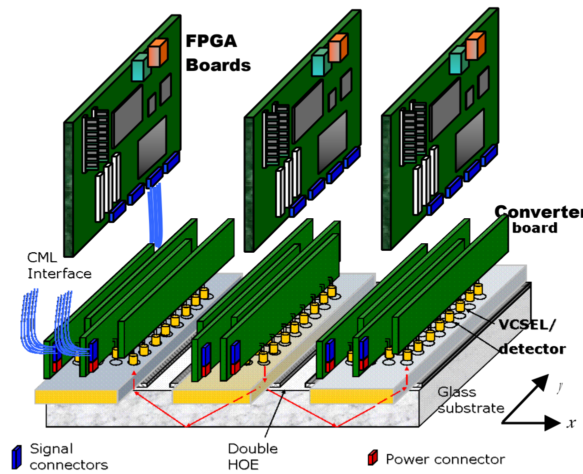

Figure 1 Diagram of optical subsystem

In Section II, the alignment tolerance will be analyzed for packaging purpose, and in Section III, the fabrication process will be illustrated. Section IV concludes the paper with performance data.

II. Packaging Orientated Alignment Tolerance Analysis

A. Optical Layer Configuration

Figure 1 illustrates that hologram film at the top surface of glass substrate works as the optical fan-in/fan-out devices so that the light signal from one board could be delivered to other boards. When the diffractive angle of the light is greater than 42°, which is the critical angle of the glass-air interface for Total Internal Reflection (TIR).

For an optical backplane bus system, the most important factors that ensure the high speed data delivery are the received optical power and noise. Therefore, the fundamental theory of the diffractive optics needs to be investigated first to ensure uniform and sufficient power delivery and low crosstalk. The Kogelnik's theory [5], is widely used because it allows analytical form of solution to be obtained.

For each of the 3 boards in the optical backplane bus shown in Fig. 1, there is a 20μm thick DuPont photopolymer (HRF-600X100-20) hologram film covering an area of 3cm×5cm between the electro-optical (EO) converter modules and the waveguiding glass substrate. Because of the centralized architecture, the central board requires a doubly multiplexed hologram [4].

The 4×8 individually packaged transceivers with 4.7mm diameter were packaged in a holding plate with 5.5mm channel pitch allocated for each computer board, to facilitate the analysis of the fan-out power uniformity among multiple channels. The thickness of the waveguiding glass substrate d is 1.5cm, which gives a reasonable slot separation of $2d$ when the diffraction angle within the substrate is exactly 45°.

There are 4 pairs of transceivers on each of the EO converter modules and all driver ICs use Current Mode Logic (CML) for interfacing with upper layer controller board through an electrical signal connector (Molex 75586-0009) with 8 pairs of differential I/O signal pins. The purpose of using electrical cable at current stage is to simplify the design of optical and electrical domain. The three upper layer controller boards provided by Advanced Communication Concepts, Inc., use Xilinx FPGA chips to verify the integrity of data transmission through PVGA.

B. Angular Bandwidth Analysis using Kogelnik's Theory

According to Kogilnik's theory [5], the diffraction efficiency and diffractive angle can be calculated using formula (1) and the diffraction efficiency gets maximum value according to formula (2) at condition (3).

$$\eta = \frac{\sin^2 \sqrt{\nu^2 + \xi^2}}{1 + \frac{\xi^2}{\nu^2}} \quad (1)$$

$$\eta = \sin^2(\nu) = \sin^2\left(\frac{\pi n_1 d}{\lambda\sqrt{c_R c_S}}\right) \quad (2)$$

$$\boldsymbol{K} = 2\beta\cos(\phi - \theta) \quad (3)$$

Approximately, the 3dB angular bandwidth is proportional to the design wavelength but inverse proportional to the thickness of hologram as shown in (4).

$$\xi_{3dB} = \frac{\vartheta d}{2c_s} = \frac{d \cdot K\sin(\phi - \theta)\cdot \partial\theta}{2c_s} \quad (4)$$

However, the desired diffractive efficiency will be always 100% to ensure good signal to noise ratio, so that the thickness of grating for longer wavelength may be reduced instead of index modulation depth. This results in a wider acceptance angle for longer operation wavelength. A 1550nm grating with n_1=0.017 and d=20μm gives an angular bandwidth of 2.7° instead of 1.4° for 850nm. As shown in Figure 2, if the thickness for 1550nm operation is increased proportionally to the wavelength, the curve of the θ_{3dB} versus maximum efficiency overlaps with that for 850nm. This analysis shows that: only if thickness of grating can be reduced using higher index modulation depth, will the tolerance be greatly improved.

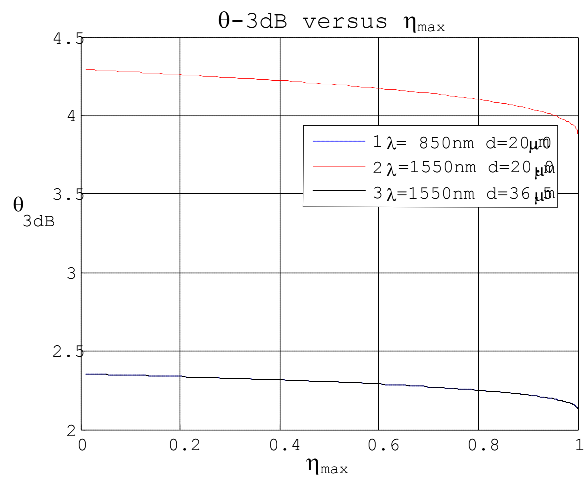

Figure 2 Curve of 3dB angular bandwidth versus desired maximum diffractive efficiency

C. Wavelength Bandwidth Analysis using Kogelnik's Theory

Operating wavelength varies for individual lasers and a screening is necessary. For λ_0=850nm, θ=0° and ϕ=67.5°, the product of n_1 and d equal to 0.3574μm will ensure 100% maximum efficiency to be obtained. Analysis shows that for wavelength greater than 850nm, the diffractive efficiency drops but the wavelength bandwidth increases, as shown in Figure 5.

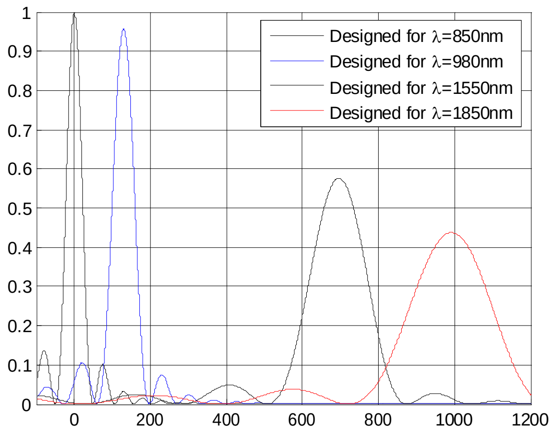

Figure 3 Wavelength Bandwidth increases with operating wavelength for hologram grating with 20µm thickness

Formula (5) shows that the 3dB wavelength bandwidth is also inverse proportional to the thickness of the grating, but proportional to the square of wavelength through variable K. The optical bandwidths of the holograms are drawn in Figure 4 showing different bandwidth and maximum diffractive efficiency at different operation wavelengths.

$$\xi_{3dB-\pi/2} = \frac{\vartheta d}{2c_s} = \frac{\partial \lambda K^2 d}{8\pi n c_s} \qquad (5)$$

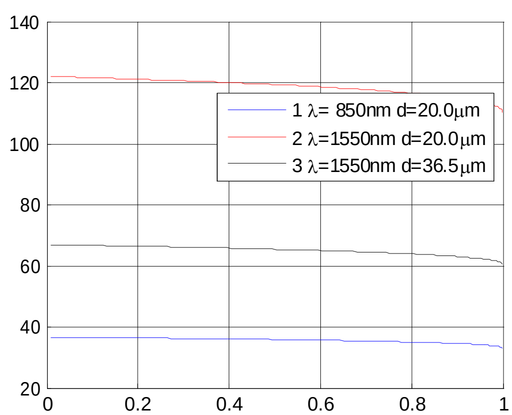

Figure 4 Relation of η_{max} and λ_{3dB} (nm) with first order approximation: only depends on the ratio of wavelength squared to grating thickness

D. System Alignment Tolerance

Figure 5 shows the transmission through a pair of 20µm thick hologram gratings for 850nm wavelength vicinity. One step of the calculation is to pre-calculate the incident angle for the fan-out coupling because the wavelength deviation causes diffractive angle to change according to formula (6).

$$n_3 \sin\theta'' = n_1 \sin\theta' - \frac{\lambda}{\Lambda}\sin\phi \qquad (6)$$

Wavelength deviation (nm)

Figure 5 Diffraction efficiency versus wavelength for TE mode: dotted line is for light with 0° incident angle, dashed line is for light with 45° incident angle and solid line for a light beam to go through a pair of hologram grating

The wavelength bandwidth is calculated to be 36nm for TE mode coupling through a pair of hologram film with mirrored fringe patters illustrated in Figure 2 for 850nm operation. The 3-dB fan-in bandwidth for 0° incident angle is around 45nm, and the bandwidth for 45° fan-out process is around 62nm.

Figure 6 shows that for an input beam with 0° incident angle but a wavelength other than the 850nm design wavelength, the diffractive angle will be different with 45°.

Diffractive angle (°)

Figure 6 Diffractive angle versus wavelength deviation for TE mode: dotted line for a scenario with 0° incident angle and dashed line for 45° incident angle.

Semiconductor laser for communication purpose usually has an output window size of 10µm to 20µm, which gives a divergence angle of around 17°. This is well beyond the angular tolerance range of the hologram film. Therefore, a collimation system has to be utilized to reduce the divergence angle. For demonstration purposes, commercially available collimators with fiber connectors to interface with connectorized transceivers and transceivers packaged with dome lenses were used in the system. The first approach is more expensive, but gives freedom to the choice of transceivers; the second approach is cheaper, but not all kind of transceivers are available with dome lens. The divergence angle for collimator output beam is about 0.5° for multimode fiber, and 0.2° for single mode fiber, while the divergence angle for dome lens is about 2°. Larger divergence angle will cause extra lost because the hologram grating gives less efficiency for large incident angle, but makes the alignment easier also because of the larger divergence. In general, it is desirable to have a thinner hologram film because angular bandwidth is inverse proportional to the grating thickness.

Experimental result shows that the detector orientation determines the detected power because the high speed detector area is very small. It can be shown from Figure 7 that if the incident angle is greater than 1.4° so that the tangent of the incident angle is greater than 100µm divided by focal length, 4mm, the focused light spot will be outside the detector active region with 100µm diameter.

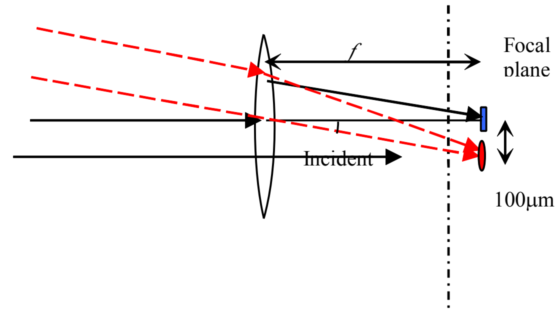

Figure 7 Illustration of detector misalignment

E. Polarization and angular bandwidth

The fan-in diffraction efficiency versus incident angle is plot in Figure 8 to show the angular dependency of TE and TM mode. From the calculation, the maximum efficiency of TM mode is only 82% while it is 100% for TE mode with same index modulation depth. However, it can be seen from the normalized TM efficiency curve that the TM mode diffractive efficiency is almost proportional to that of TE mode for different incident angle. According to this result, instead of using both TE and TM formulas, we use TE mode only in all calculations and it is accurate enough for angular bandwidth. However, the fan-in and fan-out efficiency will not reach 100% if the laser light has both TE and TM mode. In the worst case, the laser output consists equal amount of TE and TM power, the final throughput efficiency will be (100% × 100% + 82% × 82%) / (100%+100%) = 83%. Figure 9 also shows that the fan-in angular bandwidth of 0° incident angle is around 2° and it's 2.8° for fan-out, both in the film. The throughput angular bandwidth is 1.4° in the hologram and glass medium and it is equivalent to 2° in the air.

F. Dispersion Analysis

The calculated 36nm bandwidth of the hologram grating is equivalent to around 15THz when using WDM according to $df=f\cdot d\lambda/\lambda$. However, if a single laser is modulated, the bandwidth will e expanded and therefore the light will encounter diffractive efficiency loss and also the diffraction angle change. It can be calculated that the bandwidth dispersion for single channel laser pulse is about 2.5THz, same as that experimentally verified in [6].

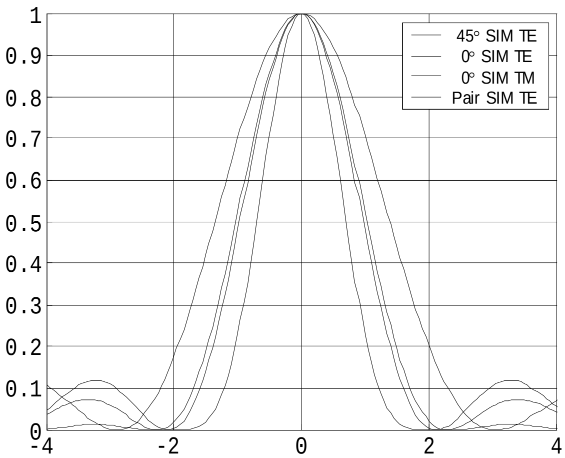

Figure 8 Diffraction efficiency versus input angle for TE and TM mode: the solid line shows TM mode which is almost proportional to TE mode in dotted line. The dashed line shows the diffractive efficiency versus deviation of incident angle around 45°.

III. DESIGN AND FABRICATION

It is necessary to test the uniformity of the large area film for multi-channel alignment. The film divergence angle of recording beam is measured to be less than 0.05° and power density profile has a 2.5cm 3dB radius. A glass substrate with a parallelism of less than 0.1° shown in Figure 9 was selected to minimize accumulated incident angle errors for the daughter boards.

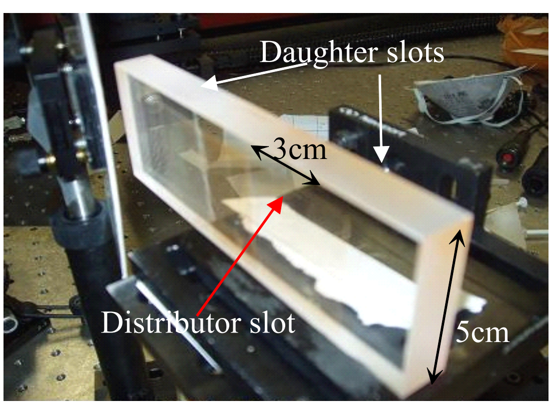

Figure 9 Hologram films on the substrate

After exposure under the 532nm laser beams for about 1 minute, the index modulation reached to the desired value. A comparison of the normalized diffraction efficiency of the hologram from theoretical calculation and from experimental measurement is shown in Figure 10. The 4° angular range between the first two minimums in our simulation for a 20μm thick hologram agrees reasonably well with the experimental measurement.

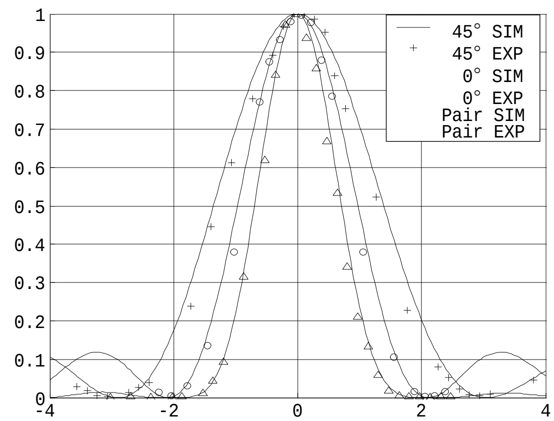

Figure 10 Calculated and measured diffraction efficiency [7]

For an optical beam to be fanned in or fanned out by a PVG with maximum efficiency, the incident angle has to satisfy the Bragg condition, and we call it Bragg incident angle. The fan-out hologram should have a mirrored fringe pattern in reference to the fan-in hologram. It is a must due to the need to broadcast data to two opposite directions.

The fabrication system was aligned so that the Bragg incident angle was maintained below 0.1°. The deviation of the Bragg condition of the incident angle along the x direction in a range of 2.5cm was also measured, as shown in Figure 11. By moving the recording stage, the probing beam can incident from different spot on the film and therefore, the diffraction efficiency on different spots can be monitored by detecting the power of diffracted light. The fact that measured η-θ_0 curves almost overlap implies that the recording beams were well collimated and the exposure was reasonably uniform all over the 3cm×5cm area.

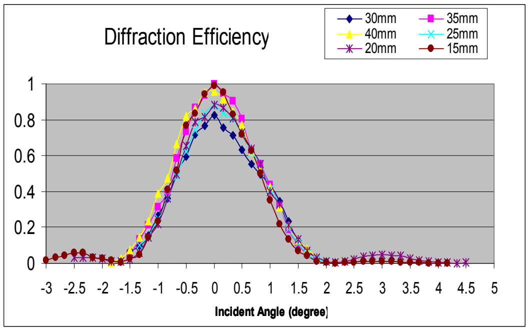

Figure 11 Measurement of incident angle deviation along horizontal direction

IV. System Packaging

A. Mechanical Packaging

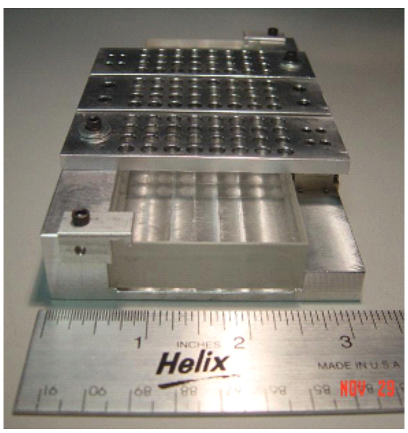

Figure 12 Photographs of the fabricated metal case for the optical backplan

A metal holding case shown in Figure 12 is fabricated for housing the glass substrate. The glass substrate and the metal plates are fixed related to the holding case. All together, there are 48 VCSELs selected with wavelength within 838 to 842nm range to be packaged into the system, because the grating is recorded using 840nm probing beam. The photo of the system with only the central slot packaged is shown in Figure 13 to show the 16-channe fan-out spots. Four circuit boards are controlling the VCSELs with equalized DC current emit equalized power, and then the power delivered to each channel is recorded. The measured result shows that there is around 3dB variation. The variation can be caused by variations of: hologram efficiency, VCSEL power-current characteristics, VCSEL wavelength, and VCSEL and detector orientation. However, 3dB is a very good result according to future analysis of the bandwidth performance of a real system.

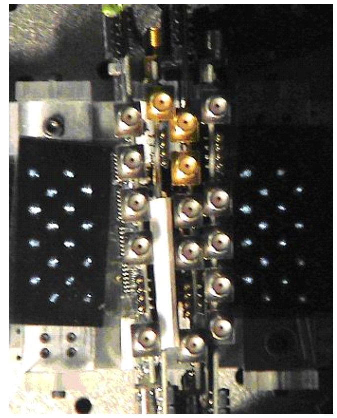

Figure 13 Photo of the fan-out beam spot of the 16-channel system

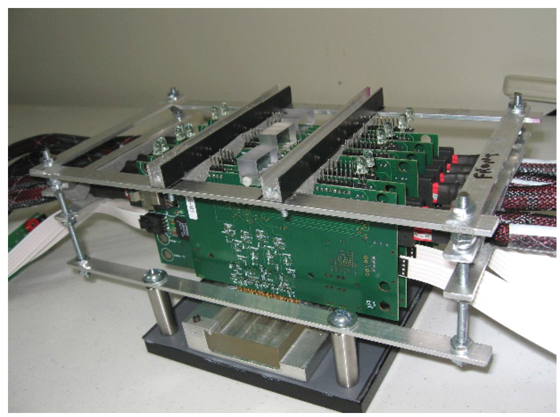

Figure 14 Packaged Optical Sub-System

B. System Performance

The fan-out power variance was measured to be less than 3dB. The variance was due to factors including VCSEL power, driver output current, and hologram efficiency distribution. The sub-system was then fully packaged as shown in Figure 14 and Figure 15.

The system was tested using FPGA chips working at 150MHz with all 32 channels sending packets. There is no error observed but some lost of packets. However, this could be due to the 8B10B encoding because even using electrical cable, same phenomena was observed.

Using a single 10Gbps VCSEL from AOC with collimators, about -10dBm optical power was delivered to both daughter boards and 10^{-12} bit error rate was estimated for 10Gbps transmission. Therefore the limit of the optical backplane bus system is also caused by the packing density of electronic and optoelectronic devices, not only the alignment.

Figure 15 Packaged Computer System using 16-Channel Optical Backplane Bus

Acknowledgment

This work was sponsored by Advanced Communications Concepts and National Security Agency.

References

[1] Ray T. Chen, L.L., Chulchae Choi, Yujie J. Liu, Bipin Bihari,L. Wu, Suning Tang, R. Wickman, B. Picor, M. K. Hibbs-Brenner, J. Bristow, And Y. S. Liu, Fully embedded board level guided-wave optoelctronic interconnects. Invited Paper, Proceedings Of IEEE. vol.88: p. pp.780-793.

[2] Dawei Huang, T.S., Anders Landin, Rick Lytel, and Howard L. Davidson, Optical interconnects: out of the box forever? IEEE Journal of Selected Topics in Quantum Electronics. vol. 9(No. 2): p. pp.614.

[3] Hai Bi, X.H., Xiaonan Chen, Jinho Choi, Wei Jiang and Ray T. Chen, "15Gbps Bit-Interleaved Optical Backplane Bus using Volume Photo-polymer Holograms". IEEE Photonics Technology Letters, Oct 2006. vol. 18(no. 21).

[4] Xuliang Han, G.K., G. Jack Lipovski, and Ray T. Chen, An Optical Centralized Shared-Bus Architecture Demonstrator for Microprocessor-to-Memory Interconnects. IEEE JOURNAL OF SELECTED TOPICS IN QUANTUM ELECTRONICS, March/April 2003. 9(2).

[5] Kogelnik, H., "Coupled wave theory for thick hologram gratings,". The Bell System Technical Journal, November 1969. vol. 48(no. 9): p. pp. 2909-2947.

[6] Gicherl Kim, R.T.C., "Three-dimensionally interconnected bidirectional optical backplane," IEEE Photonics Technology Letters, July 1999. vol. 11(no. 7): p. pp. 880-882.

[7] Hai Bi, J.C., Wei Jiang, Xuliang Han, Jonathan Ellis and Ray T. Chen, 3.2Gbps multi-channel optical backplane bus demonstrator using photopolymer volume gratings. Proc. SPIE 6478-11, Jan 2007.